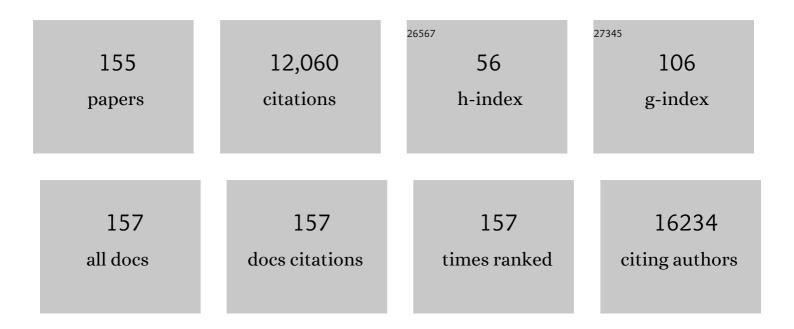
Kai Xiao

List of Publications by Year in descending order

Source: https://exaly.com/author-pdf/2587459/publications.pdf Version: 2024-02-01



KAL XIAO

#	Article	IF	CITATIONS
1	Understanding Heterogeneities in Quantum Materials. Advanced Materials, 2023, 35, e2106909.	11.1	8
2	Selective Antisite Defect Formation in WS ₂ Monolayers via Reactive Growth on Dilute Wâ€Au Alloy Substrates. Advanced Materials, 2022, 34, e2106674.	11.1	14
3	Atomic Edge-Guided Polyethylene Crystallization on Monolayer Two-Dimensional Materials. Macromolecules, 2022, 55, 559-567.	2.2	6
4	Nonequilibrium synthesis and processing approaches to tailor heterogeneity in 2D materials. , 2022, , 221-258.		1
5	Janus Monolayers for Ultrafast and Directional Charge Transfer in Transition Metal Dichalcogenide Heterostructures. ACS Nano, 2022, 16, 4197-4205.	7.3	18
6	Laser synthesis and processing of atomically thin 2D materials. Trends in Chemistry, 2022, 4, 769-772.	4.4	1
7	Stabilized Synthesis of 2D Verbeekite: Monoclinic PdSe ₂ Crystals with High Mobility and In-Plane Optical and Electrical Anisotropy. ACS Nano, 2022, 16, 13900-13910.	7.3	14
8	Heterogeneities at multiple length scales in 2D layered materials: From localized defects and dopants to mesoscopic heterostructures. Nano Research, 2021, 14, 1625-1649.	5.8	8
9	Controllable Thinâ€Film Approaches for Doping and Alloying Transition Metal Dichalcogenides Monolayers. Advanced Science, 2021, 8, 2004249.	5.6	51
10	Strain-Induced Growth of Twisted Bilayers during the Coalescence of Monolayer MoS ₂ Crystals. ACS Nano, 2021, 15, 4504-4517.	7.3	19
11	Understanding Substrate-Guided Assembly in van der Waals Epitaxy by <i>in Situ</i> Laser Crystallization within a Transmission Electron Microscope. ACS Nano, 2021, 15, 8638-8652.	7.3	7
12	Phase segregation mechanisms of small moleculeâ€polymer blends unraveled by varying polymer chain architecture. SmartMat, 2021, 2, 367-377.	6.4	18
13	Designing Atomic Edge Structures in 2D Transition Metal Dichalcogenides for Improved Catalytic Activity. Microscopy and Microanalysis, 2021, 27, 964-965.	0.2	0
14	Atomic-scale Feedback-controlled Electron Beam Fabrication of 2D Materials. Microscopy and Microanalysis, 2021, 27, 3072-3073.	0.2	0
15	Automatic detection of crystallographic defects in STEM images by unsupervised learning with translational invariance. Microscopy and Microanalysis, 2021, 27, 1460-1462.	0.2	1
16	Inside Front Cover: Volume 2 Issue 3. SmartMat, 2021, 2, iii.	6.4	0
17	Excitonic Dynamics in Janus MoSSe and WSSe Monolayers. Nano Letters, 2021, 21, 931-937.	4.5	86
18	Defect detection in atomic-resolution images via unsupervised learning with translational invariance. Npj Computational Materials, 2021, 7, .	3.5	11

#	Article	IF	CITATIONS
19	Magnetostriction of α-RuCl ₃ Flakes in the Zigzag Phase. Journal of Physical Chemistry C, 2021, 125, 25687-25694.	1.5	2
20	Defects in Highly Anisotropic Transition-Metal Dichalcogenide PdSe ₂ . Journal of Physical Chemistry Letters, 2020, 11, 740-746.	2.1	28
21	Investigation of Structural Phases in Mo1-xWxTe2 in STEM. Microscopy and Microanalysis, 2020, 26, 2362-2364.	0.2	0
22	Twoâ€Dimensional Palladium Diselenide with Strong Inâ€Plane Optical Anisotropy and High Mobility Grown by Chemical Vapor Deposition. Advanced Materials, 2020, 32, e1906238.	11.1	81
23	Low Energy Implantation into Transition-Metal Dichalcogenide Monolayers to Form Janus Structures. ACS Nano, 2020, 14, 3896-3906.	7.3	136
24	Anisotropic Phonon Response of Few‣ayer PdSe ₂ under Uniaxial Strain. Advanced Functional Materials, 2020, 30, 2003215.	7.8	26
25	Atomically Precise PdSe2 Pentagonal Nanoribbons. ACS Nano, 2020, 14, 1951-1957.	7.3	21
26	Twin domains modulate light-matter interactions in metal halide perovskites. APL Materials, 2020, 8, .	2.2	17
27	In situ laser reflectivity to monitor and control the nucleation and growth of atomically thin 2D materials*. 2D Materials, 2020, 7, 025048.	2.0	14
28	Relationship between the Nature of Monovalent Cations and Charge Recombination in Metal Halide Perovskites. ACS Applied Energy Materials, 2020, 3, 1298-1304.	2.5	11
29	Layer-by-Layer Thinning of PdSe ₂ Flakes via Plasma Induced Oxidation and Sublimation. ACS Applied Materials & Interfaces, 2020, 12, 7345-7350.	4.0	20
30	Connecting Femtosecond Transient Absorption Microscopy with Spatially Coregistered Time Averaged Optical Imaging Modalities. Journal of Physical Chemistry A, 2020, 124, 3915-3923.	1.1	4
31	Electronâ€Beamâ€Related Studies of Halide Perovskites: Challenges and Opportunities. Advanced Energy Materials, 2020, 10, 1903191.	10.2	53
32	The role of mid-gap phonon modes in thermal transport of transition metal dichalcogenides. Journal of Physics Condensed Matter, 2020, 32, 025306.	0.7	3
33	Lightâ€Ferroic Interaction in Hybrid Organic–Inorganic Perovskites. Advanced Optical Materials, 2019, 7, 1901451.	3.6	24
34	lsotope-Engineering the Thermal Conductivity of Two-Dimensional MoS ₂ . ACS Nano, 2019, 13, 2481-2489.	7.3	42
35	Deep learning analysis of defect and phase evolution during electron beam-induced transformations in WS2. Npj Computational Materials, 2019, 5, .	3.5	113
36	Strain tolerance of two-dimensional crystal growth on curved surfaces. Science Advances, 2019, 5, eaav4028.	4.7	46

#	Article	IF	CITATIONS
37	Atomic Insight into Thermolysisâ€Driven Growth of 2D MoS ₂ . Advanced Functional Materials, 2019, 29, 1902149.	7.8	28
38	Defect-Mediated Phase Transformation in Anisotropic Two-Dimensional PdSe ₂ Crystals for Seamless Electrical Contacts. Journal of the American Chemical Society, 2019, 141, 8928-8936.	6.6	81
39	Spatial Mapping of Thermal Boundary Conductance at Metal–Molybdenum Diselenide Interfaces. ACS Applied Materials & Interfaces, 2019, 11, 14418-14426.	4.0	16
40	Lithographically patterned metallic conduction in single-layer MoS2 via plasma processing. Npj 2D Materials and Applications, 2019, 3, .	3.9	21
41	Synthesis and emerging properties of 2D layered III–VI metal chalcogenides. Applied Physics Reviews, 2019, 6, 041312.	5.5	89
42	Exploring the air stability of PdSe2 via electrical transport measurements and defect calculations. Npj 2D Materials and Applications, 2019, 3, .	3.9	55
43	Reply to: On the ferroelectricity of CH3NH3PbI3 perovskites. Nature Materials, 2019, 18, 1051-1053.	13.3	21
44	A roadmap for electronic grade 2D materials. 2D Materials, 2019, 6, 022001.	2.0	205
45	On the origin of spatially dependent electronic excited-state dynamics in mixed hybrid perovskite thin films. Lithuanian Journal of Physics, 2019, 58, .	0.1	2
46	Tip-induced local strain on <mml:math xmlns:mml="http://www.w3.org/1998/Math/MathML"> <mml:mrow> <mml:mi>Mo</mml:mi> <mml:msub> <mm mathvariant="normal">S <mml:mn>2</mml:mn> </mm </mml:msub> <mml:mo>/</mml:mo> <mml:mi>grapl detected by inelastic electron tunneling spectroscopy. Physical Review B, 2018, 97, .</mml:mi></mml:mrow></mml:math 	:mi 1,1 nite <td>mi>⁶/mml:mrc</td>	mi> ⁶ /mml:mrc
47	Effect of Charge Localization on the Effective Hyperfine Interaction in Organic Semiconducting Polymers. Physical Review Letters, 2018, 120, 086602.	2.9	32
48	In Situ X-Ray Studies of Crystallization Kinetics and Ordering in Functional Organic and Hybrid Materials. , 2018, , 33-60.		0
49	Realâ€Time Observation of Orderâ€Disorder Transformation of Organic Cations Induced Phase Transition and Anomalous Photoluminescence in Hybrid Perovskites. Advanced Materials, 2018, 30, e1705801.	11.1	60
50	Anomalous interlayer vibrations in strongly coupled layered PdSe ₂ . 2D Materials, 2018, 5, 035016.	2.0	60
51	The growth and assembly of organic molecules and inorganic 2D materials on graphene for van der Waals heterostructures. Carbon, 2018, 131, 246-257.	5.4	21
52	Effect of Metal Doping and Vacancies on the Thermal Conductivity of Monolayer Molybdenum Diselenide. ACS Applied Materials & Interfaces, 2018, 10, 4921-4928.	4.0	29
53	High-performance multilayer WSe2 field-effect transistors with carrier type control. Nano Research, 2018, 11, 722-730.	5.8	101
54	Ultrafast Exciton Dissociation at the 2D-WS ₂ Monolayer/Perovskite Interface. Journal of Physical Chemistry C, 2018, 122, 28910-28917.	1.5	23

#	Article	IF	CITATIONS
55	Laser Synthesis, Processing, and Spectroscopy of Atomically-Thin Two Dimensional Materials. Springer Series in Materials Science, 2018, , 1-37.	0.4	1
56	Atmospheric and Long-term Aging Effects on the Electrical Properties of Variable Thickness WSe ₂ Transistors. ACS Applied Materials & Interfaces, 2018, 10, 36540-36548.	4.0	31
57	Transformation of 2D group-III selenides to ultra-thin nitrides: enabling epitaxy on amorphous substrates. Nanotechnology, 2018, 29, 47LT02.	1.3	6
58	Impact of Crystallographic Orientation Disorders on Electronic Heterogeneities in Metal Halide Perovskite Thin Films. Nano Letters, 2018, 18, 6271-6278.	4.5	22
59	Valence band inversion and spin-orbit effects in the electronic structure of monolayer GaSe. Physical Review B, 2018, 98, .	1.1	47
60	In situ edge engineering in two-dimensional transition metal dichalcogenides. Nature Communications, 2018, 9, 2051.	5.8	100
61	Mapping mesoscopic phase evolution during E-beam induced transformations via deep learning of atomically resolved images. Npj Computational Materials, 2018, 4, .	3.5	31
62	Chemical nature of ferroelastic twin domains in CH3NH3PbI3 perovskite. Nature Materials, 2018, 17, 1013-1019.	13.3	183
63	Dynamic behavior of CH3NH3PbI3 perovskite twin domains. Applied Physics Letters, 2018, 113, .	1.5	27
64	3D Imaging and Manipulation of Subsurface Selenium Vacancies in <mml:math xmlns:mml="http://www.w3.org/1998/Math/MathML" display="inline"><mml:mrow><mml:msub><mml:mrow><mml:mi>PdSe</mml:mi></mml:mrow><mml:mrow>< Physical Review Letters, 2018, 121, 086101.</mml:mrow></mml:msub></mml:mrow></mml:math 	mmi:mn>2	</td
65	Photocarrier Transfer across Monolayer MoS ₂ –MoSe ₂ Lateral Heterojunctions. ACS Nano, 2018, 12, 7086-7092.	7.3	25
66	In situ atomistic insight into the growth mechanisms of single layer 2D transition metal carbides. Nature Communications, 2018, 9, 2266.	5.8	125
67	lon Migration Studies in Exfoliated 2D Molybdenum Oxide via Ionic Liquid Gating for Neuromorphic Device Applications. ACS Applied Materials & Interfaces, 2018, 10, 22623-22631.	4.0	12
68	Transition Metal Dichalcogenides: Suppression of Defects and Deep Levels Using Isoelectronic Tungsten Substitution in Monolayer MoSe ₂ (Adv. Funct. Mater. 19/2017). Advanced Functional Materials, 2017, 27, .	7.8	3
69	Enhancing Ion Migration in Grain Boundaries of Hybrid Organic–Inorganic Perovskites by Chlorine. Advanced Functional Materials, 2017, 27, 1700749.	7.8	74
70	Edge-Controlled Growth and Etching of Two-Dimensional GaSe Monolayers. Journal of the American Chemical Society, 2017, 139, 482-491.	6.6	65
71	Synthesis and Photoluminescence Properties of 2D Phenethylammonium Lead Bromide Perovskite Nanocrystals. Small Methods, 2017, 1, 1700245.	4.6	27
72	PdSe ₂ : Pentagonal Two-Dimensional Layers with High Air Stability for Electronics. Journal of the American Chemical Society, 2017, 139, 14090-14097.	6.6	509

#	Article	IF	CITATIONS
73	High Conduction Hopping Behavior Induced in Transition Metal Dichalcogenides by Percolating Defect Networks: Toward Atomically Thin Circuits. Advanced Functional Materials, 2017, 27, 1702829.	7.8	52
74	Atomic Defects and Edge Structure in Single-layer Ti ₃ C ₂ T _x MXene. Microscopy and Microanalysis, 2017, 23, 1704-1705.	0.2	7
75	Tilt Grain Boundary Topology Induced by Substrate Topography. ACS Nano, 2017, 11, 8612-8618.	7.3	27
76	Deep Learning of Atomically Resolved Scanning Transmission Electron Microscopy Images: Chemical Identification and Tracking Local Transformations. ACS Nano, 2017, 11, 12742-12752.	7.3	282
77	Nonequilibrium Synthesis of TiO ₂ Nanoparticle "Building Blocks―for Crystal Growth by Sequential Attachment in Pulsed Laser Deposition. Nano Letters, 2017, 17, 4624-4633.	4.5	33
78	Separating Bulk and Surface Contributions to Electronic Excited-State Processes in Hybrid Mixed Perovskite Thin Films via Multimodal All-Optical Imaging. Journal of Physical Chemistry Letters, 2017, 8, 3299-3305.	2.1	20
79	Tunable quasiparticle band gap in few-layer GaSe/graphene van der Waals heterostructures. Physical Review B, 2017, 96, .	1.1	99
80	Suppression of Defects and Deep Levels Using Isoelectronic Tungsten Substitution in Monolayer MoSe ₂ . Advanced Functional Materials, 2017, 27, 1603850.	7.8	84
81	High performance top-gated multilayer WSe ₂ field effect transistors. Nanotechnology, 2017, 28, 475202.	1.3	33
82	2D materials advances: from large scale synthesis and controlled heterostructures to improved characterization techniques, defects and applications. 2D Materials, 2016, 3, 042001.	2.0	408
83	Low thermal budget, photonic-cured compact TiO ₂ layers for high-efficiency perovskite solar cells. Journal of Materials Chemistry A, 2016, 4, 9685-9690.	5.2	46
84	Imaging Electronic Trap States in Perovskite Thin Films with Combined Fluorescence and Femtosecond Transient Absorption Microscopy. Journal of Physical Chemistry Letters, 2016, 7, 1725-1731.	2.1	48
85	Atomic Defects in Monolayer Titanium Carbide (Ti ₃ C ₂ T _{<i>x</i>}) MXene. ACS Nano, 2016, 10, 9193-9200.	7.3	785
86	Persistent photoconductivity in two-dimensional Mo _{1â^'<i>x</i>} W _{<i>x</i>} Se ₂ –MoSe ₂ van der Waals heterojunctions. Journal of Materials Research, 2016, 31, 923-930.	1.2	20
87	Ultrafast Dynamics of Metal Plasmons Induced by 2D Semiconductor Excitons in Hybrid Nanostructure Arrays. ACS Photonics, 2016, 3, 2389-2395.	3.2	42
88	Isoelectronic Tungsten Doping in Monolayer MoSe ₂ for Carrier Type Modulation. Advanced Materials, 2016, 28, 8240-8247.	11.1	85
89	Unraveling the Fundamental Mechanisms of Solvent-Additive-Induced Optimization of Power Conversion Efficiencies in Organic Photovoltaic Devices. ACS Applied Materials & Interfaces, 2016, 8, 20220-20229.	4.0	8
90	Patterned Growth of Pâ€Type MoS ₂ Atomic Layers Using Sol–Gel as Precursor. Advanced Functional Materials, 2016, 26, 6371-6379.	7.8	34

#	Article	IF	CITATIONS
91	Tailoring Vacancies Far Beyond Intrinsic Levels Changes the Carrier Type and Optical Response in Monolayer MoSe _{2â^'<i>x</i>} Crystals. Nano Letters, 2016, 16, 5213-5220.	4.5	121
92	Two-dimensional GaSe/MoSe ₂ misfit bilayer heterojunctions by van der Waals epitaxy. Science Advances, 2016, 2, e1501882.	4.7	239
93	Ultrafast Charge Transfer and Hybrid Exciton Formation in 2D/0D Heterostructures. Journal of the American Chemical Society, 2016, 138, 14713-14719.	6.6	102
94	Observation of Nanoscale Morphological and Structural Degradation in Perovskite Solar Cells by in Situ TEM. ACS Applied Materials & Interfaces, 2016, 8, 32333-32340.	4.0	54
95	Nanoforging Single Layer MoSe2 Through Defect Engineering with Focused Helium Ion Beams. Scientific Reports, 2016, 6, 30481.	1.6	82
96	Interlayer Coupling in Twisted WSe ₂ /WS ₂ Bilayer Heterostructures Revealed by Optical Spectroscopy. ACS Nano, 2016, 10, 6612-6622.	7.3	249
97	Low temperature synthesis of hierarchical TiO ₂ nanostructures for high performance perovskite solar cells by pulsed laser deposition. Physical Chemistry Chemical Physics, 2016, 18, 27067-27072.	1.3	29
98	Twisted MoSe ₂ Bilayers with Variable Local Stacking and Interlayer Coupling Revealed by Low-Frequency Raman Spectroscopy. ACS Nano, 2016, 10, 2736-2744.	7.3	117
99	Separation of Distinct Photoexcitation Species in Femtosecond Transient Absorption Microscopy. ACS Photonics, 2016, 3, 434-442.	3.2	18
100	Deciphering Halogen Competition in Organometallic Halide Perovskite Growth. Journal of the American Chemical Society, 2016, 138, 5028-5035.	6.6	92
101	Simplification of femtosecond transient absorption microscopy data from CH ₃ NH ₃ PbI ₃ perovskite thin films into decay associated amplitude maps. Nanotechnology, 2016, 27, 114002.	1.3	11
102	Thickness-dependent charge transport in few-layer MoS ₂ field-effect transistors. Nanotechnology, 2016, 27, 165203.	1.3	124
103	Ultrathin nanosheets of CrSiTe ₃ : a semiconducting two-dimensional ferromagnetic material. Journal of Materials Chemistry C, 2016, 4, 315-322.	2.7	235
104	Nanophase Engineering of Organic Semiconductor-Based Solar Cells. Springer Series in Materials Science, 2016, , 197-228.	0.4	3
105	Observation of two distinct negative trions in tungsten disulfide monolayers. Physical Review B, 2015, 92, .	1.1	44
106	Peculiarity of Two Thermodynamically-Stable Morphologies and Their Impact on the Efficiency of Small Molecule Bulk Heterojunction Solar Cells. Scientific Reports, 2015, 5, 13407.	1.6	16
107	Controllable Growth of Perovskite Films by Roomâ€Temperature Air Exposure for Efficient Planar Heterojunction Photovoltaic Cells. Angewandte Chemie - International Edition, 2015, 54, 14862-14865.	7.2	41
108	Revealing the Preferred Interlayer Orientations and Stackings of Twoâ€Dimensional Bilayer Gallium Selenide Crystals. Angewandte Chemie, 2015, 127, 2750-2755.	1.6	5

#	Article	IF	CITATIONS
109	Quantitative Phase Fraction Detection in Organic Photovoltaic Materials through EELS Imaging. Polymers, 2015, 7, 2446-2460.	2.0	16
110	High-Performance Flexible Perovskite Solar Cells by Using a Combination of Ultrasonic Spray-Coating and Low Thermal Budget Photonic Curing. ACS Photonics, 2015, 2, 680-686.	3.2	268
111	Ultrahigh photo-responsivity and detectivity in multilayer InSe nanosheets phototransistors with broadband response. Journal of Materials Chemistry C, 2015, 3, 7022-7028.	2.7	203
112	Revealing the Preferred Interlayer Orientations and Stackings of Twoâ€Dimensional Bilayer Gallium Selenide Crystals. Angewandte Chemie - International Edition, 2015, 54, 2712-2717.	7.2	45
113	Van der Waals Epitaxial Growth of Two-Dimensional Single-Crystalline GaSe Domains on Graphene. ACS Nano, 2015, 9, 8078-8088.	7.3	103
114	Elucidation of Perovskite Film Micro-Orientations Using Two-Photon Total Internal Reflectance Fluorescence Microscopy. Journal of Physical Chemistry Letters, 2015, 6, 3283-3288.	2.1	24
115	Patterned arrays of lateral heterojunctions within monolayer two-dimensional semiconductors. Nature Communications, 2015, 6, 7749.	5.8	213
116	Perovskite Solar Cells with Near 100% Internal Quantum Efficiency Based on Large Single Crystalline Grains and Vertical Bulk Heterojunctions. Journal of the American Chemical Society, 2015, 137, 9210-9213.	6.6	246
117	Spatial Localization of Excitons and Charge Carriers in Hybrid Perovskite Thin Films. Journal of Physical Chemistry Letters, 2015, 6, 3041-3047.	2.1	59
118	Correlating high power conversion efficiency of PTB7:PC ₇₁ BM inverted organic solar cells with nanoscale structures. Nanoscale, 2015, 7, 15576-15583.	2.8	54
119	Low-Frequency Raman Fingerprints of Two-Dimensional Metal Dichalcogenide Layer Stacking Configurations. ACS Nano, 2015, 9, 6333-6342.	7.3	151
120	Perovskites: transforming photovoltaics, a mini-review. Journal of Photonics for Energy, 2015, 5, 057402.	0.8	47
121	The isotopic effects of deuteration on optoelectronic properties of conducting polymers. Nature Communications, 2014, 5, 3180.	5.8	103
122	Pulsed Laser Deposition of Photoresponsive Twoâ€Đimensional GaSe Nanosheet Networks. Advanced Functional Materials, 2014, 24, 6365-6371.	7.8	108
123	Digital Transfer Growth of Patterned 2D Metal Chalcogenides by Confined Nanoparticle Evaporation. ACS Nano, 2014, 8, 11567-11575.	7.3	47
124	Highly sensitive phototransistors based on two-dimensional GaTe nanosheets with direct bandgap. Nano Research, 2014, 7, 694-703.	5.8	140
125	Understanding How Processing Additives Tune the Nanoscale Morphology of High Efficiency Organic Photovoltaic Blends: From Casting Solution to Spun ast Thin Film. Advanced Functional Materials, 2014, 24, 6647-6657.	7.8	39
126	Controlled Vapor Phase Growth of Single Crystalline, Two-Dimensional GaSe Crystals with High Photoresponse. Scientific Reports, 2014, 4, 5497.	1.6	222

ΚΑΙ ΧΙΑΟ

#	Article	IF	CITATIONS
127	Laser Interactions for the Synthesis and In Situ Diagnostics of Nanomaterials. Springer Series in Materials Science, 2014, , 143-173.	0.4	4
128	High-performance organic field-effect transistors with dielectric and active layers printed sequentially by ultrasonic spraying. Journal of Materials Chemistry C, 2013, 1, 4384.	2.7	27
129	High-performance polymer photovoltaics based on rationally designed fullerene acceptors. Solar Energy Materials and Solar Cells, 2013, 118, 171-178.	3.0	25
130	Conjugated Polymer-Mediated Polymorphism of a High Performance, Small-Molecule Organic Semiconductor with Tuned Intermolecular Interactions, Enhanced Long-Range Order, and Charge Transport. Chemistry of Materials, 2013, 25, 4378-4386.	3.2	77
131	Solvent quality-induced nucleation and growth of parallelepiped nanorods in dilute poly(3-hexylthiophene) (P3HT) solution and the impact on the crystalline morphology of solution-cast thin film. CrystEngComm, 2013, 15, 1114-1124.	1.3	51
132	Surface-Induced Orientation Control of CuPc Molecules for the Epitaxial Growth of Highly Ordered Organic Crystals on Graphene. Journal of the American Chemical Society, 2013, 135, 3680-3687.	6.6	125
133	Correlation of polymeric compatibilizer structure to its impact on the morphology and function of P3HT:PCBM bulk heterojunctions. Journal of Materials Chemistry A, 2013, 1, 5309.	5.2	33
134	Highly Responsive Ultrathin GaS Nanosheet Photodetectors on Rigid and Flexible Substrates. Nano Letters, 2013, 13, 1649-1654.	4.5	683
135	Morphological origin for the stratification of P3HT:PCBM blend film studied by neutron reflectometry. Applied Physics Letters, 2013, 103, .	1.5	14
136	The impact of controlled solvent exposure on the morphology, structure and function of bulk heterojunction solar cells. Solar Energy Materials and Solar Cells, 2012, 107, 112-124.	3.0	48
137	Exciton–Exciton Annihilation in Copper-phthalocyanine Single-Crystal Nanowires. Journal of Physical Chemistry C, 2012, 116, 21588-21593.	1.5	15
138	Understanding the Metal-Directed Growth of Single-Crystal M-TCNQF ₄ Organic Nanowires with Time-Resolved, in Situ X-ray Diffraction and First-Principles Theoretical Studies. Journal of the American Chemical Society, 2012, 134, 14353-14361.	6.6	17
139	Synthesis of Few-Layer GaSe Nanosheets for High Performance Photodetectors. ACS Nano, 2012, 6, 5988-5994.	7.3	788
140	Ternary behavior and systematic nanoscale manipulation of domain structures in P3HT/PCBM/P3HT-b-PEO films. Journal of Materials Chemistry, 2012, 22, 13013.	6.7	53
141	High-Performance Field-Effect Transistors Based on Polystyrene- <i>b</i> -Poly(3-hexylthiophene) Diblock Copolymers. ACS Nano, 2011, 5, 3559-3567.	7.3	122
142	Enhanced Performance Consistency in Nanoparticle/TIPS Pentaceneâ€Based Organic Thin Film Transistors. Advanced Functional Materials, 2011, 21, 3617-3623.	7.8	81
143	PSâ€ <i>b</i> â€P3HT Copolymers as P3HT/PCBM Interfacial Compatibilizers for High Efficiency Photovoltaics. Advanced Materials, 2011, 23, 5529-5535.	11.1	110
144	Reduced Grain Size and Improved Thermoelectric Properties of Melt Spun (Hf,Zr)NiSn Half-Heusler Alloys. Journal of Electronic Materials, 2010, 39, 2008-2012.	1.0	58

#	Article	IF	CITATIONS
145	Metastable Copperâ€Phthalocyanine Singleâ€Crystal Nanowires and Their Use in Fabricating Highâ€Performance Fieldâ€Effect Transistors. Advanced Functional Materials, 2009, 19, 3776-3780.	7.8	81
146	Growth, Patterning, and One-Dimensional Electron -Transport Properties of Self-Assembled Ag-TCNQF4 Organic Nanowires. Chemistry of Materials, 2009, 21, 4275-4281.	3.2	48
147	Selective Patterned Growth of Singleâ€Crystal Ag–TCNQ Nanowires for Devices by Vapor–Solid Chemical Reaction. Advanced Functional Materials, 2008, 18, 3043-3048.	7.8	57
148	One-dimensional electron transport in Cu-tetracyanoquinodimethane organic nanowires. Applied Physics Letters, 2007, 90, 193115.	1.5	22
149	Single-Crystal Organic Nanowires of Copper–Tetracyanoquinodimethane: Synthesis, Patterning, Characterization, and Device Applications. Angewandte Chemie - International Edition, 2007, 46, 2650-2654.	7.2	90
150	A Highly π-Stacked Organic Semiconductor for Field-Effect Transistors Based on Linearly Condensed Pentathienoacene. Journal of the American Chemical Society, 2005, 127, 13281-13286.	6.6	334
151	Thin-Film Transistors Based on Langmuirâ dlodgett Films of Heteroleptic Bis(phthalocyaninato) Rare Earth Complexes. Langmuir, 2005, 21, 6527-6531.	1.6	68
152	Multiwall nanotubes with intramolecular junctions (CNx/C): Preparation, rectification, logic gates, and application. Applied Physics Letters, 2004, 84, 4932-4934.	1.5	28
153	Field-Effect Transistors Based on Langmuirâ^Blodgett Films of Phthalocyanine Derivatives as Semiconductor Layers. Journal of Physical Chemistry B, 2003, 107, 9226-9230.	1.2	73
154	High performance field-effect transistors made of a multiwall CNx/C nanotube intramolecular junction. Applied Physics Letters, 2003, 83, 4824-4826.	1.5	23
155	Molecular Scaffold Growth of Two-Dimensional, Strong Interlayer-Bonding-Layered Materials. CCS Chemistry, 0, , 117-127.	4.6	10